

The Discovery of Orally Active Triaminotriazine Aniline Amides as Inhibitors of p38 MAP Kinase

Katerina Leftheris,^{*,†} Gulzar Ahmed,[‡] Ran Chan,[‡] Alaric J. Dyckman,[†] Zahid Hussain,[‡] Kan Ho,[‡] John Hynes, Jr.,[†] Jeffrey Letourneau,[‡] Wei Li,[‡] Shuqun Lin,[†] Axel Metzger,[‡] Kevin J. Moriarty,[‡] Chris Riviello,[‡] Yvonne Shimshock,[‡] James Wen,[‡] John Wityak,[†] Stephen T. Wroblewski,[†] Hong Wu,[†] Junjun Wu,[‡] Madhuri Desai,[‡] Kathleen M. Gillooly,[§] Tsung H. Lin,[‡] Derek Loo,[§] Kim W. McIntyre,[§] Sidney Pitt,[§] Ding Ren Shen,[§] David J. Shuster,[§] Rosemary Zhang,[§] David Diller,[‡] Arthur Doweiko,^{||} John Sack,^{||} Jack Baldwin,[‡] Joel Barrish,[†] John Dodd,[†] Ian Henderson,[‡] Steve Kanner,[§] Gary L. Schieven,[§] and Maria Webb[‡]

Departments of Chemistry, Biology and Modeling, Pharmacoepia, Departments of Discovery Chemistry, Macromolecular Structure, and Immunology, Bristol-Myers Squibb, PO Box 4000, Princeton, New Jersey 08543-4000

Received June 18, 2004

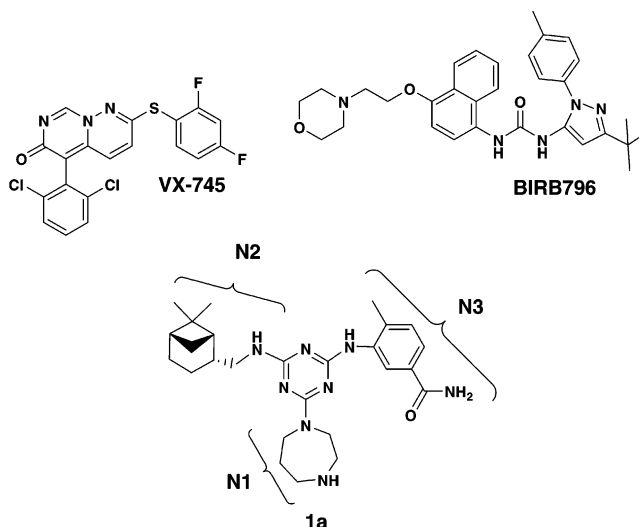
A new structural class of triaminotriazine aniline amides possessing potent p38 enzyme activity has been discovered. The initial hit (compound **1a**) was identified through screening the Pharmacoepia ECLiPS compound collection. SAR modification led to the identification of a short acting triaminotriazine aniline methoxyamide (compound **1m**) possessing in vitro and in vivo oral activity in animal models of acute and chronic inflammatory disease. An X-ray crystal structure of compound **1m** in this class, cocrystallized with unactivated p38 α protein, indicates that these compounds bind to the ATP binding pocket and possess key H-bonding interactions within a deeper cleft. Hydrogen bonding between one of the triazine nitrogens and the backbone NH of the Met109 residue occurs through a water molecule. The methoxyamide NH and carbonyl oxygen are within H-bonding distance of Glu71 and Asp168.

Introduction

Overproduction of cytokines such as IL-1 and TNF- α are implicated in a wide variety of inflammatory diseases, including rheumatoid arthritis (RA), psoriasis, multiple sclerosis, inflammatory bowel disease, endotoxic shock, osteoporosis, Alzheimer's disease, and congestive heart failure, among others.¹ There is significant clinical proof of concept demonstrating that reduction of systemic circulating levels of these key inflammatory mediators is beneficial in the treatment of inflammatory diseases such as rheumatoid arthritis, Crohn's disease, and psoriasis. Examples of these agents include the soluble TNF- α receptor Fc fusion protein (etanercept), anti-TNF antibody (infliximab), and the IL-1 receptor antagonist (anakinra).²

The stress-activated signal transduction pathway leading to inflammatory cytokine production in stimulated immune cells is known to be regulated in part by p38 α mitogen activated protein (MAP) kinase. p38 MAP kinase is a member of a Ser-Thr kinase superfamily that includes p38, ERK2, and JNK.³ There are four known isoforms of p38: p38 α and p38 β are widely expressed in eukaryotic cells including endothelial and inflammatory cells. Expression of p38 γ is found in skeletal muscle, and p38 δ is predominantly expressed in the small intestine, kidney, and lung tissue.⁴ p38 α is part of a stress-activated intracellular signaling cascade. Activation of the cascade occurs through external stimuli

Chart 1



such as osmotic stress, inflammatory cytokines, heat, and UV light. Once activated, p38 α phosphorylates intracellular substrates such as MAPKAP K2, which in turn regulate the biosynthesis of TNF α and IL-1 β at the posttranscriptional level.

Targeting TNF α and IL-1 β through inhibition of p38 α with an orally active small molecule inhibitor represents an attractive alternative to current biologic therapy. There is potential for lower cost of goods, oral vs parenteral administration, lower patient costs, and suppression of both TNF α and IL-1 β with monotherapy.

Numerous companies have efforts in pursuing p38 α inhibitors for the treatment of inflammatory disease. VX-745 (Chart 1) advanced to phase II trials and reported a correlation between p38 inhibition and an

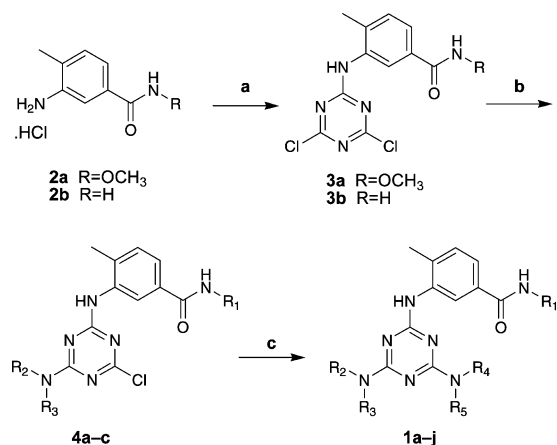
* To whom correspondence should be addressed: Bristol-Myers Squibb, PO Box 4000, Princeton, NJ 08543-4000. Phone: (609)-252-6188. Fax: (609)-252-7410. E-mail: katerina.leftheris@bms.com.

[†] Department of Discovery Chemistry.

[‡] Departments of Chemistry, Biology and Modeling, Pharmacoepia.

[§] Department of Immunology.

^{||} Department of Macromolecular Structure.

Scheme 1^a

^a Conditions: (a) cyanuric chloride, (iPr)₂NEt, acetone, 0 °C; (b) R₂R₃NH₂⁺Cl⁻, (iPr)₂NEt, THF, 0 °C to room temperature or R₂R₃NH, THF, 0 °C to room temperature; (c) R₄R₅NH, *N*-methylpyrrolidinone, 80 °C.

antiinflammatory effect in RA patients before it was discontinued. VX-702 (structure not disclosed) is currently in clinical trials for acute coronary syndrome.⁵ BIRB-796 is currently in clinical trials for several antiinflammatory indications.⁶ In designing inhibitors, there has been an emphasis on identifying molecules that bind at least in part to the ATP binding pocket of p38 as well as accessing allosteric sites.^{5,7}

Herein, we describe our initial efforts in developing potent, selective 1,3,5-triaminotriazine aniline amides as inhibitors of p38 α MAP kinase through iterative SAR studies. Our initial hit **1a** was identified through screening the Pharmacopeia ECLiPS compound collection.

Design and Synthesis

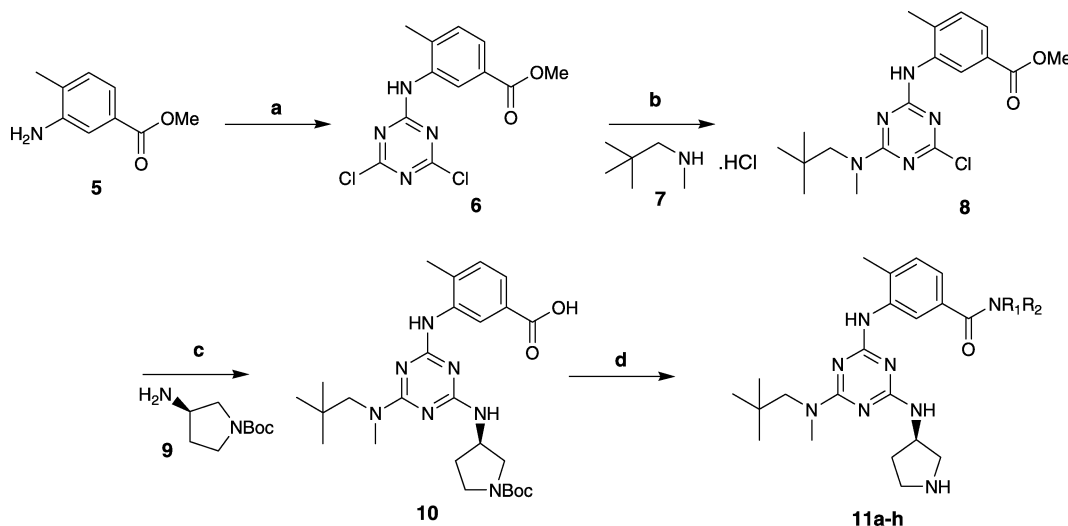
As shown in Scheme 1, the desired aniline amide **2** was first coupled to cyanuric chloride through direct chloride displacement to form **3**. Order of addition of substituents onto the triazine core can occur in several ways. Due to the relatively poor nucleophilicity of

anilines compared to aliphatic amines, coupling of the desired aniline to cyanuric chloride was selected first. This was followed by subsequent couplings of the desired amines under basic conditions to form the corresponding triaminotriazines **1a–n**. For aminopyrrolidine-containing derivatives, the aminopyrrolidine was coupled as the Boc-protected amine (**9**, Scheme 2) to avoid formation of the incorrect regioisomer. For several members of this series, modification of the aniline was desired while maintaining the pyrrolidine and the neopentyl(methyl) amino side chains. Therefore, the aniline was coupled as the methyl 3-amino-4-methylbenzoate (**5**). Ester hydrolysis to the carboxylic acid followed by amide coupling and Boc deprotection of the pyrrolidine occurred after the triaminotriazine was constructed.

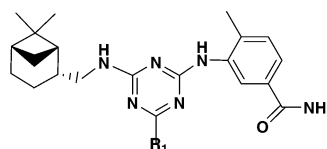
Discussion

Compounds were evaluated for their ability to inhibit phosphorylation of substrate (myelin basic protein) by recombinant human p38 α . A THP-1 assay was used to measure the ability of compounds to inhibit LPS-induced TNF production in cells.

The triaminotriazine inhibitor hit (**1a**) possesses three potential sites for SAR modification (N1, N2, and N3). We utilized an SAR strategy for identifying potent p38 α inhibitors that involved altering substituents at one site while the remaining sites were held constant. As shown in Table 1, initial efforts focused on exploring modification of the 1,4-diazepan ring of **1a** to determine if other aliphatic ring systems containing a basic residue are tolerated. Conversion to the methylated derivative **1b** did not alter enzyme activity. Replacement of the 1,4-diazepan by NH₂ (**1c**) led to a compound with a slight reduction in enzyme inhibition. However, introduction of the amino pyrrolidine ring (**1d**) improved enzyme inhibitory potency by 25-fold. However, cell activity was not significantly improved over that of the parent. Chirality of the pyrrolidine ring does not appear to play a role in enzyme inhibition or cell activity since the corresponding (*S*)-pyrrolidine demonstrated similar po-

Scheme 2^a

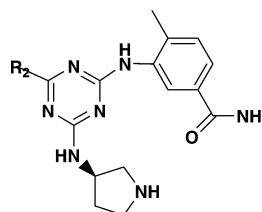
^a Conditions: (a) cyanuric chloride, acetone, 0 °C, 98%; (b) **7**, (iPr)₂NEt, THF, 0 °C to room temperature, 98%; (c) (i) **9**, *N*-methylpyrrolidinone, 80–140 °C; (ii) aqueous NaOH, MeOH, 79%; (d) (i) EDCI, HOBt, R₁R₂NH, room temperature; (ii) HCl, dioxane, room temperature 22–88%.

Table 1. Selected Substituted Triaminotriazines **1a–d**


The structure shows a 1,3,5-triazine ring with an N1-substituent (R1), an N2-substituent (a myrtanyl group), and an N3-substituent (a 3-amino-4-methylbenzamide group).

R ₁	p38α IC ₅₀ (nM) ^a	TNFα (THP-1) IC ₅₀ (nM) ^b
1a 1,4-diazepan-1-yl	1360	1700
1b 1,4-diazepan-1-yl(methyl)	1420	nd
1c NH ₂	5900	nd
1d (<i>R</i>)-pyrrolidine-3-ylamino	53	1100

^a *n* = 4, variation in individual values, <20%. ^b *n* = 3, variation in individual values, <25%.

Table 2. Selected Triaminotriazine R₂ Replacements **1e–j**


The structure shows a 1,3,5-triazine ring with an N1-substituent (R2), an N2-substituent (a pyrrolidine group), and an N3-substituent (a 3-amino-4-methylbenzamide group).

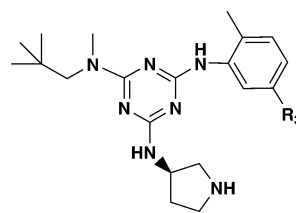
R	p38α IC ₅₀ (nM) ^a	TNFα (THP-1) IC ₅₀ (nM) ^b
1e <i>p</i> -fluorophenethylamino	227	>5000
1f 2-phenylpropyl(methyl)amino	84	2600
1g 2-methylpropylamino	73	>5000
1h 2-methylpropyl(methyl)amino	28	325
1i neopentylmethyl(methyl)amino	24	167
1j cyclohexylmethyl(methyl)amino	250	1300

^a *n* = 4, variation in individual values, <20%. ^b *n* = 3, variation in individual values, <25%.

tency (data not shown). Therefore, the R configuration of the pyrrolidine was chosen for subsequent SAR studies.

As shown in Table 2, modification of the myrtanyl group at N2 was explored while maintaining the (*R*)-pyrrolidine at N1 and 3-amino-4-methylbenzamide at N3. Introduction of aromatic substituents (**1e**) or aliphatic substituents (**1g**) led to potent inhibitors of the p38 enzyme. However, cell activity remained modest. Introduction of a methyl group in addition to the hydrophobic substituents at N2 (thereby forming a tertiary amine) gave a dramatic improvement in cell activity. The increase in cell permeability on methylation may be due to the increase in overall hydrophobicity. Comparison of **1g** (without methyl) vs **1h** (with methyl) shows a 3-fold improvement in enzyme inhibition and >10-fold improvement in cell activity. Further branching of the side chain leads to **1i**, the most potent compound in this series.

With N1 and N2 optimized ((*R*)-pyrrolidine and neopentyl(methyl)amino, respectively), modification of N3 was undertaken (Table 3). Modifications of the 2-methyl of the aniline to include conservative changes such as F, Cl, and methoxy are tolerated (data not shown). However, introduction of additional functional groups to the aniline aromatic ring or any of the methyl regioisomers led to a significant drop in enzyme inhibition. This was also true for the 5-amido substituent. Modifications such as introduction of the amide in any position other than the 5 position led to a >100-fold

Table 3. Selected Triaminotriazine R₃ Replacements **11a–h**


The structure shows a 1,3,5-triazine ring with an N1-substituent (a neopentyl(methyl)amino group), an N2-substituent (a pyrrolidine group), and an N3-substituent (R3).

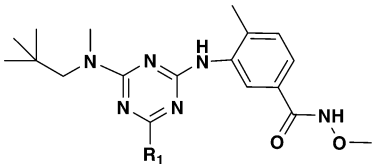
R ₃	p38α IC ₅₀ (nM) ^a	TNFα (THP-1) IC ₅₀ (nM) ^b
11a CONH ₂	31	140
11b CONHCH ₂ CH ₂ OCH ₃	264	680
11c CONHBn	64	85
11d COOCH ₃	346	>250
11e CONHcyclopentyl	100	130
11f CONHOCH ₃	8	16
11g CONHOH	16	150
11h CONHCH(CH ₃) ₂	51	150

^a *n* = 4, variation in individual values, <20%. ^b *n* = 3, variation in individual values, <25%.

reduction in enzyme inhibition. Therefore, focus was placed on conservative changes where positioning of the 2-methyl and the 5-amido were not altered. Simple alkyl amides in place of CONH₂ are well tolerated. As shown for **11a**, both enzyme and cell activity are equivalent compared to **1i**. Branching of the alkyl group (**11h**) is also well tolerated. Introduction of longer chains including an alkoxy group results in a 9-fold reduction in enzyme inhibition (**11b**). Benzyl as well as cyclopentyl groups are tolerated (**11c**, **11e**). However, a methyl ester results in greater than a 10-fold reduction in enzyme potency. Introduction of a methoxyamide (**11f**) leads to a 4-fold improvement in enzyme and >9-fold improvement in cell activity vs **11a**. The electron withdrawing capability of the alkoxy group in alkoxyamides may contribute to improving the H-bonding capability of the amide NH. The hydroxamic acid **11g** also displays potent enzyme activity. However, cell activity is diminished compared to **11f** potentially due to the impact this group may have on the overall hydrophobicity of the molecule. Other alkoxyamides are well tolerated. However, as seen for the alkyl amides, extension beyond an ethyl group leads to compounds with diminished enzyme activity (data not shown). Because of the improvement in enzyme and cell activity, the 1-amino-2-methyl-5-(*N*-methoxy)benzamide was chosen as a key functionality for the N3 position.

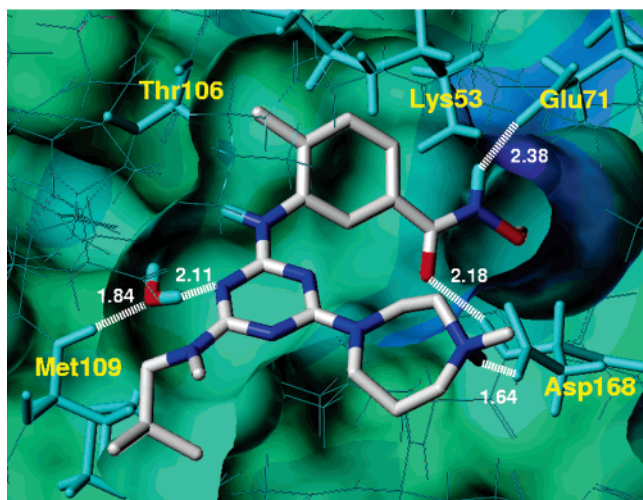
Table 4 shows further modification of N1 where N3 contains the aniline methoxyamide. The optimal compound in this series based on cell activity (**1m**) contains a 1,4-diazepan-1-yl group where the terminal amine is methylated.

The X-ray crystal structure of **1m** bound to unphosphorylated p38α enzyme was examined for key binding interactions. The p38-bound **1m** ligand exhibits several key hydrogen-bonding contacts in the ATP binding pocket (Figure 1). A distinct contact occurs between the triazine nitrogen and Met109 backbone NH through a water molecule (NH–O, 1.84 Å; OH–N, 2.11 Å). In most other kinase inhibitors accessing the ATP pocket, contact with Met109 backbone NH occurs directly with a ligand heteroatom. The pendant methoxyamide ester NH and carbonyl oxygen are within hydrogen-bonding distance of Glu71 (2.38 Å) and Asp168 (2.18 Å, backbone

Table 4. Optimization of R₁ **1k–n**


R ₁	p38α IC ₅₀ (nM) ^a	TNFα (THP-1) IC ₅₀ (nM) ^b	
1k	4-methylpiperazine-1-yl	57	158
1l	piperazine-1-yl	18	120
1m	4-methyl-1,4-diazepan-1-yl	44	85
1n	1,4-diazepan-1-yl	52	131

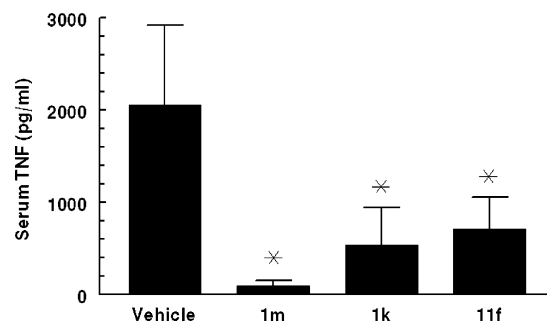
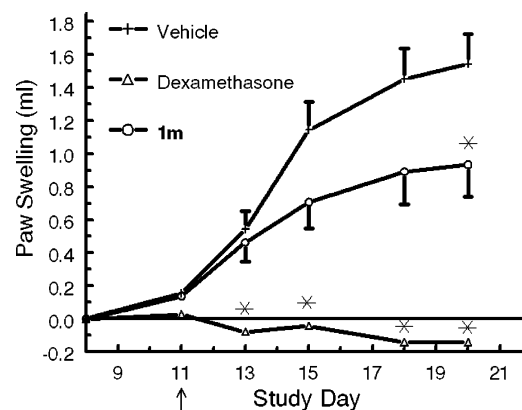
^a $n = 4$, variation in individual values, <20%. ^b $n = 3$, variation in individual values, <25%.

**Figure 1.** X-ray crystal structure of **1m** cocrystallized with p38 protein.

NH), respectively. In addition, the *N*-methyl portion of the 1,4-diazepan ring is located near Asp168 (1.64 Å), suggesting that the protonated amine may form a salt bridge with the Asp168 anion. Two hydrophobic interactions are evident as well. The angular aniline fits well within the classic hydrophobic pocket located distal to Thr106, while the *N*-neopentyl group lies along the hinge region.

To determine the *in vivo* efficacy profile, several compounds were screened for oral activity in an acute model of TNFα inhibition (murine LPS/TNF model). Mice were dosed with 3 compounds (**11f**, **1k**, and **1m**) at 5 mg/kg (po) 30 min prior to LPS administration. TNF levels were measured after 90 min. As shown in Figure 2, **1m** showed near complete suppression of TNF levels. Other compounds suppressed TNF levels but not to the same extent. The ED₅₀ for **1m** in this model was determined to be 3–10 mpk. A time course study was undertaken where **1m** was dosed at time intervals from 30 min to 10 h prior to LPS challenge at 10 mpk (data not shown). Suppression of TNF diminished when the compound was dosed 6 h prior to LPS challenge. However, the compound was active at 30 min and 2 h prior to LPS challenge. Further evaluation of **1m** in a model of chronic inflammation (adjuvant arthritis rat) demonstrated 50% suppression of paw swelling when dosed at 50 mg/kg, (b.i.d., po) (Figure 3).

Further profiling of **1m** was undertaken to determine characteristics of the compound as well as potential

**Figure 2.** LPS-induced TNF inhibition of several p38 inhibitors in mouse. For oral dosing, compounds were prepared in a solution of 100% polyethylene glycol (MW 300) and a dosing volume of 0.2 mL per mouse (BALB/c female mice, 6–8 weeks of age) was administered by gavage 30 min prior to LPS injection (0.1 mL of LPS suspended at 10 μg/mL in PBS, administered ip). Blood samples were obtained 90 min after LPS injection. Serum was separated from clotted blood samples by centrifugation (5 min, 5000g, room temperature) and analyzed for levels of TNF-α by ELISA assay (R&D Systems) according to the manufacturer's directions. Results are shown as mean ± SD of $n = 8$ mice per treatment group.**Figure 3.** Rat adjuvant arthritis study using **1m**. Lewis rats ($n = 8$ /group) were immunized with complete Freund's adjuvant on day 0. On day 11, twice-daily oral treatment was initiated with vehicle (Tween80:ethanol:water, 5:5:90) or **1m** (50 mg/kg/dose; circles). Dexamethasone (0.5 mg/kg; triangles) given orally once daily was used as a positive control. Hind paw volume increases were determined by plethysmometry on the days indicated. * = $p < 0.05$ vs vehicle, Student's *t* test.**Table 5.** Kinase Selectivity Profile of Compound **1m**

kinase	kinase assay (IC ₅₀ , μM)	kinase	kinase assay (IC ₅₀ , μM)
p38α	0.004 (K_i)	PKA	> 10
p38β	0.022	LCK	> 10
IKK2β	> 10	SYK	> 10
MK2	> 10	Zap70	> 50
JAK3	> 10	KDR	> 10
PKCα,δ	> 10		

liabilities. The K_i of **1m** was determined to be 4.2 nM. LPS-induced TNF production in human peripheral blood mononuclear cells (hPBMC) gave an IC₅₀ of 4.6 nM. A difference in IC₅₀ between hPBMC and THP-1 (transformed cell line) may reflect a difference in dependence on p38 in mediating TNF levels in different cell types. A cytotoxicity assay using PHA blast cells demonstrated minimal toxicity (70% of control when treated for 24 h at 30 μM), and kinase profiling of **1m** (Table 5) did not identify significant off target kinase activity. However,

there is little kinase selectivity between p38 α and p38 β for **1m**.

The rate of metabolism of **1m** in liver microsomes is high for mouse (0.8 nmol/min/mg protein) and human (0.2 nmol/min/mg protein). The major metabolite observed in both species is the carboxylic acid formed from the methoxyamide by hydrolysis. Consequently, the PK profile for this compound in mouse shows a high clearance (6.4 L/h·kg), short $T_{1/2}$ (0.7 h), and low bioavailability (8% BA). Nonetheless, oral efficacy was observed for **1m** in in vivo rodent models of acute and chronic inflammation. In vivo efficacy was shown not to be due to formation of an active metabolite since the corresponding carboxylic acid hydrolysis product showed very low p38 enzyme activity ($>1 \mu\text{M}$).

Conclusions

In conclusion, we have identified novel triaminotriazine aniline methoxyamides as potent, orally active p38 inhibitors. One member of this class (**1m**) demonstrates efficacy in a chronic inflammatory disease model, shows significant kinase selectivity, is not cytotoxic, and possesses a PK profile synonymous with a short acting compound. X-ray crystallography demonstrates that this compound accesses the ATP binding pocket of p38, forming a hydrogen bond through a water molecule to the backbone NH of Met109. The aniline methoxyamide plays a key role in accessing a deeper cleft through hydrogen-bonding interactions with Glu71 and Asp168. The triaminotriazine aniline methoxyamides, as exemplified by **1m**, represent an attractive starting point for the design and synthesis of potent and selective p38 inhibitors with superior pharmacokinetic profiles. Given the toxicity issues p38 inhibitors have had in development, a highly potent, short acting p38 inhibitor may provide the desired efficacy needed with minimal adverse effects. However, appropriate pharmacokinetic and pharmacodynamic studies will be required to fully understand the profile needed to maximize in vivo efficacy as well as therapeutic index.

Experimental Section

Chemistry. Proton magnetic resonance (^1H NMR) spectra were recorded on a Bruker ARX-400 spectrometer and are reported in ppm relative to the reference solvent of the sample in which they were run. HPLC and LCMS analyses were conducted using a Shimadzu LC-10AS liquid chromatograph and a SPD UV-vis detector at 220 nm with the MS detection performed with a Micromass Platform LC spectrometer. HPLC analyses were performed using the following conditions: Ballistic YMC S5 ODS 4.6×50 mm column with a binary solvent system where solvent A = 10% methanol, 90% water, 0.2% phosphoric acid and solvent B = 90% methanol, 10% water, and 0.2% phosphoric acid, flow rate = 4 mL/min, linear gradient time = 4 min, start %B = 0, final %B = 100.

LCMS analyses were performed using the following conditions: Waters Xterra $5 \mu\text{M}$ 4.6×30 mm column with a binary solvent system where solvent A = 10% methanol, 90% water, 0.1% trifluoroacetic acid and solvent B = 90% methanol, 10% water, and 0.1% trifluoroacetic acid, flow rate = 4 mL/min, linear gradient time = 2 min, start %B = 0, final %B = 100. HPLC purification was performed using a YMC column (SH-345-15, S-15, 120A ODS, 20×500 mm) with acetonitrile:water gradients containing 0.1% trifluoroacetic acid. All reagents were purchased from commercial sources and used without further purification unless otherwise noted. All reactions were performed under an inert atmosphere. Reactions run in

aqueous media were run under an ambient atmosphere unless otherwise noted.

General Procedure for the Synthesis of Compounds 3a and 3b. Example: 3-(4,6-Dichloro-1,3,5-triazin-2-ylamino)-*N*-methoxy-4-methylbenzamide (3a). To a solution of 3-amino-*N*-methoxy-4-methylbenzamide (5.4 mmol, **2a**)⁸ in acetone (20 mL) at 0 °C was added 1.0 g (5.4 mmol) of cyanuric chloride, and the resulting mixture was stirred at 0 °C for 2 h and then at room temperature for an additional 2 h. Crushed ice (~10 mL) was added, and the mixture was allowed to warm to room temperature over 1 h. The solid was collected by vacuum filtration and was washed with water (3×10 mL). Drying in vacuo afforded the title compound as a white solid in 90% yield. ^1H NMR (400 MHz, MeOD₄): δ 7.75 (d, J = 1.5 Hz, 1H), 7.65 (dd, J = 7.7, 1.6 Hz, 1H), 7.41 (d, J = 8.2 Hz, 1H), 3.82 (s, 3H), 2.32 (s, 3H). HPLC: t_{R} = 2.43 min, 95% purity.

3-(4,6-Dichloro-1,3,5-triazin-2-ylamino)-4-methylbenzamide (3b). This compound was prepared according to the procedure for **3a** starting with 4-methylbenzamide (**2b**).⁸ Yield: 89%, white solid. ^1H NMR (400 MHz, DMSO-*d*₆): δ 11.17 (s, 1H), 10.80 (s, 1H), 7.94–7.32 (m, 4H), 2.24 (s, 3H). HPLC: t_{R} = 2.89 min, 92.3% purity. LCMS (EI): m/z calcd for C₁₁H₉N₅O [M + H]⁺ 298.10, found 298.05.

3-(4-Chloro-6-(methyl(neopentyl)amino)-1,3,5-triazin-2-ylamino)-*N*-methoxy-4-methylbenzamide (4a). To a solution of **3a** (3.1 mmol) in THF (10 mL) at 0 °C were successively added 1.2 mL (6.7 mmol) of diisopropylethylamine and neopentyl(methyl)amine hydrochloride (6.2 mmol). The resulting mixture was stirred at 0 °C for 30 min and then at room temperature for 30 min before quenching with a 50% saturated aqueous solution of ammonium chloride (15 mL). The organic solvent was removed in vacuo using a rotary evaporator, and the resulting mixture was extracted with ethyl acetate (3×20 mL). The combined extracts were washed with brine (10 mL), dried over anhydrous sodium sulfate, filtered, concentrated, and dried in vacuo to afford the title compound as a white solid in 94% yield. ^1H NMR (400 MHz, MeOD₄, appears as 2 rotamers): δ 8.20, 7.99 (br s, 1H), 7.55–7.49 (m, 1H), 7.37–7.34 (m, 1H), 3.81 (s, 3H), 3.52, 3.40 (s, 2H), 3.15, 3.14 (s, 3H), 2.36, 2.33 (s, 3H), 0.99, 0.81 (s, 9H). HPLC: t_{R} = 3.73 min, 92% purity.

3-(4-Chloro-6-(((1*S*,2*R*,5*S*)-6,6-dimethylbicyclo[3.1.1]heptan-2-yl)methylamino)-1,3,5-triazin-2-ylamino)-4-methylbenzamide (4b). This compound was prepared according to the procedure for **4a** starting with **3b** and (*S*)-myrtanylamine. Yield: 72%, white solid. ^1H NMR (400 MHz, CDCl₃, rotameric): δ 8.42 (s, 1H), 7.52 (d, J = 7.8 Hz, 1H), 7.28 (m, 1H), 6.90 (s, 1H), 3.39 (m, 2H), 2.35 (s, 3H), 2.24 (m, 1H), 1.92 (m, 4H), 1.60 (s, 6H), 1.52 (m, 1H), 1.25 (m, 3H). HPLC: t_{R} = 4.31 min, 98.7% purity. HRMS (EI): m/z calcd for C₂₁H₂₇N₆ClO [M + H]⁺ 415.2013, found 415.2017.

(*S*)-tert-Butyl-3-(4-(5-carbamoyl-2-methylphenylamino)-6-chloro-1,3,5-triazin-2-ylamino)pyrrolidine-1-carboxylate (4c). To a solution of **3b** (100 mg, 0.34 mmol) in THF (1.5 mL) at 0 °C was added DIPEA (65 μL , 0.37 mmol) followed by (*R*)-3-amino-1-*N*-Boc-pyrrolidine (86 μL , 0.37 mmol), and the solution was warmed to room temperature. The solution was stirred for 30 min, filtered, and concentrated to a semisolid. Water (2 mL) was added, and the resulting solids were stirred for 2 h, filtered off, and washed with water to give the chloro analogue **4c** as a white solid (60 mg, 39% yield). ^1H NMR (400 MHz, CDCl₃, rotameric): δ 8.32 (m, 1H), 7.54 (m, 1H), 7.28 (m, 2H), 6.30 (m, 3H), 3.45 (m, 4H), 2.24 (m, 3H), 1.92 (m, 1H), 1.45 (s, 9H). HPLC: t_{R} = 3.76 min, 95.0% purity. LCMS (EI): m/z calcd for C₂₀H₂₆N₇ClO₃ [M + H]⁺ 448.92, found 448.32.

3-(4-(((1*S*,2*R*,5*S*)-6,6-dimethylbicyclo[3.1.1]heptan-2-yl)methylamino)-6-(4-methyl-1,4-diazepan-1-yl)-1,3,5-triazin-2-ylamino)-4-methylbenzamide Trifluoroacetate (1b). A solution of **4b** (0.38 mmol) and 4-methyl-1,4-diazepan (1.9 mmol) in NMP (0.3 mL) was heated at 80 °C for 30 min. The mixture was cooled to room temperature and diluted with methanol (1 mL). This solution was subjected to purification by reverse-

phase HPLC chromatography, the HPLC fractions containing the purified title compounds were concentrated on a rotary evaporator to remove the methanol solvent, and the resulting aqueous solutions were lyophilized to afford **1b** as a tan solid. Yield: 40%. ¹H NMR (500 MHz, MeOD₄, rotameric): δ 8.06–8.18(m, 1H), 7.62–7.75(m, 1H), 7.33–7.43(m, 1H), 3.79–4.01(m, 3H), 3.30–3.60 (m, 5H), 2.94 (br s, 3H), 2.38–2.44 (m, 2H), 2.37 (br s, 3H), 2.15–2.26 (m, 2H), 1.88–2.05 (m, 7H), 1.52–1.64 (m, 1H), 1.23 (br s, 3H), 1.09 (br s, 3H), 0.92–0.98 (m, 1H) ppm. HPLC: *t*_R = 2.36 min, 95% purity. LCMS: *m/z* calcd for C₂₇H₄₀N₈O [M + H]⁺ 493.34, found 493.31.

3-(4-Amino-6-((1*S*,2*R*,5*S*)-6,6-dimethylbicyclo[3.1.1]heptan-2-yl)methylamino)-1,3,5-triazin-2-ylamino)-4-methylbenzamide (1c). To a solution of 46 mg (0.1 mmol) of **4b** in EtOH (1.3 mL) was added 0.2 mL of concentrated NH₄OH. The resulting mixture was heated at 150 °C for 60 min in a sealed tube and then cooled to room temperature. EtOH was removed, water (1 mL) was added, and the resulting solids were stirred for 24 h, filtered off, and rinsed with water. The solids were purified via column chromatography (EtOAc, then 1% MeOH/EtOAc) to afford 28.3 mg (65%) of **4d** as a white solid. ¹H NMR (400 MHz, DMSO-*d*₆): δ 8.17–7.87 (m, 3H), 7.58 (d, *J* = 7.7 Hz, 1H), 7.28 (s, 2H), 6.69 (s, 1H), 6.23 (s, 1H), 6.11 (s, 1H), 3.19 (m, 2H), 2.61 (m, 2H), 2.56 (s, 3H), 2.28 (br m, 5H), 1.87–0.86 (m, 8H). HPLC: *t*_R = 3.42 min, 99.0% purity. HRMS (EI): *m/z* calcd for C₂₁H₂₇N₇O [M + H]⁺ 396.2512, found 396.2513.

3-(4-((1*S*,2*R*,5*S*)-6,6-Dimethylbicyclo[3.1.1]heptan-2-yl)methylamino)-6-((*S*)-pyrrolidin-3-ylamino)-1,3,5-triazin-2-ylamino)-4-methylbenzamide Trifluoroacetate (1d). To a solution of chloride **4b** (45 mg, 0.1 mmol) in NMP (0.8 mL) was added (*R*)-3-amino-1-*N*-Boc-pyrrolidine (0.03 mL, 0.11 mmol) and DIPEA (0.05 mL, 0.22 mmol), and the solution was heated at 100 °C for 4 h. The solution was removed from heating, and water (2 mL) was slowly added. The precipitated solids were stirred for 1 h, filtered off, and rinsed with water to afford the Boc-protected intermediate.

To the solids was added 4 N HCl in dioxane (1.5 mL), and the solution was stirred for 2.5 h at room temperature. The solvent was removed in vacuo, and the crude solids were purified via preparative HPLC to afford the compound **1d** (32 mg, 64% yield) as a white solid. ¹H NMR (400 MHz, DMSO-*d*₆, rotameric): δ 7.95 (m, 3H), 7.45 (s, 1H), 7.15 (s, 2H), 6.86–6.32 (m, 2H), 4.15 (m, 1H), 3.41–3.07 (m, 4H), 2.76 (m, 1H), 2.61–1.74 (m, 13 H), 1.47–0.74 (m, 5H). HPLC: *t*_R = 3.07 min, 99.2% purity. HRMS (EI): *m/z* calcd for C₂₅H₃₆N₈O [M + H]⁺ 464.3012, found 464.3156.

(S)-3-(4-(4-Fluorophenethylamino)-6-(pyrrolidin-3-ylamino)-1,3,5-triazin-2-ylamino)-4-methylbenzamide Trifluoroacetate (1e). To a solution of chloride **4c** (50 mg, 0.1 mmol) in EtOAc (0.8 mL) were added 4-fluorophenethylamine (69 mg, 0.5 mmol) and Na₂CO₃ (0.046 mL, 0.22 mmol), and the solution was heated at 130 °C for 20 min. The solution was removed from heating, and water (2 mL) was slowly added. The product was extracted with CH₂Cl₂, dried over Na₂SO₄, filtered, and concentrated to an oil.

To the solids were then added CH₂Cl₂ (2 mL) and TFA (0.2 mL), and the solution was stirred for 3 h at room temperature. The solvents were then removed in vacuo and the crude solids purified via preparative HPLC to afford the compound **1e** (30 mg, 64% yield) as a white solid. ¹H NMR (400 MHz, MeOD₄, rotameric): δ 8.02 (m, 1H), 7.74 (m, 1H), 7.42 (s, 1H), 7.29 (s, 1H), 7.02 (m, 3H), 4.85 (m, 1H), 4.00 (s, 1H), 3.76–3.34 (m, 4H), 2.92 (br s, 2H), 2.41 (br s, 1H), 2.37 (s, 3H), 2.13 (br s, 1H). HPLC: *t*_R = 2.45 min, 95.3% purity. HRMS (EI): *m/z* calcd for C₂₃H₂₇N₈O [M + H]⁺ 451.2370, found 451.2366.

4-Methyl-3-(4-(methyl(2-phenylpropyl)amino)-6-((*S*)-pyrrolidin-3-ylamino)-1,3,5-triazin-2-ylamino)benzamide Trifluoroacetate (1f). To a solution of 0.5 mL (3.4 mmol) of 2-methylphenethylamine in THF (15 mL) at 0 °C was added 0.5 mL of TEA (3.4 mmol) followed by 0.75 mg of Boc₂O (3.4 mmol). The reaction mixture was stirred for 10 min and then concentrated in vacuo to an oil. The residue was dissolved in EtOAc (50 mL) and washed with 0.5 N HCl (20 mL) and

water (25 mL). The organic layer was dried over Na₂SO₄, filtered, and concentrated to an oil, which was used without further purification. ¹H NMR (400 MHz, CDCl₃): δ 7.19–7.34 (m, 5H), 4.40 (br s, 1H), 3.39 (m, 1H), 3.18 (ddd, *J* = 5.1, 8.3, 13.5 Hz, 1H), 2.92 (m, 1H), 1.41 (s, 9H), 1.26 (d, *J* = 7.0 Hz, 3H). HPLC: *t*_R = 3.96 min, 92.8% purity. LCMS: *m/z* calcd for C₁₄H₂₁N₂O₂ [M + H]⁺ 236.16, found 236.24. To a solution of 0.4 g (1.7 mmol) of *tert*-butyloxycarbonyl-2-methylphenethylamine in THF (5 mL) at 0 °C was added 0.1 g of NaH (3.4 mmol, 60% in oil) in one portion. The solution was stirred at room temperature for 2 h followed by the addition of methyl iodide 0.5 mL (8.5 mmol). After 1 h, DMF (2 mL) was added and the reaction mixture stirred for 18 h. An additional equivalent of NaH (70 mg) was added and the reaction mixture stirred for an additional 3 h. The reaction was quenched with NH₄Cl (saturated aqueous, 1 mL), poured into EtOAc (25 mL), and washed with water and brine. The organic layer was dried over Na₂SO₄, filtered, and concentrated to an oil. To the oil was added 4 N HCl in dioxane (3 mL), and the reaction mixture was stirred for 30 min. The solvent was removed and the crude solid dried under vacuum to give 2-methylphenethyl-(methyl)amine hydrochloride as a white solid, which was used without further purification. ¹H NMR (400 MHz, MeOD₄): δ 7.31–7.18 (m, 5H), 3.56 (s, 2H), 3.13 (m, 1H), 2.56 (s, 3H), 1.25 (d, *J* = 6.9 Hz, 3H). HPLC: *t*_R = 0.87 min, 93.8% purity. LCMS: *m/z* calcd for C₁₀H₁₅N [M + H]⁺ 150.20, found 150.16.

1f was prepared similarly to **1e** starting from chloride **4c** (40 mg, 0.09 mmol) and 2-methylphenethyl(methyl)amine hydrochloride (20 mg, 0.1 mmol). Yield of **1f** as a white solid: 21 mg, 52% yield: ¹H NMR (400 MHz, MeOD₄, rotameric): δ 8.05 (br m, 1H), 7.55 (m, 1H), 7.20 (m, 9H), 4.88 (s, 1H), 3.88 (m, 1H), 3.68–3.04 (m, 4H), 2.88 (s, 3H), 2.37 (s, 3H), 2.24 (s, 1H), 1.91 (s, 1H), 1.31 (s, 3H), 1.29–0.88 (m, 3H). HPLC: *t*_R = 2.68 min, 97.8% purity. HRMS (EI): *m/z* calcd for C₂₅H₃₂N₈O [M + H]⁺ 461.2777, found 461.2781.

(S)-3-(4-(Isopropylamino)-6-(pyrrolidin-3-ylamino)-1,3,5-triazin-2-ylamino)-4-methylbenzamide Trifluoroacetate (1g). **1g** was prepared similarly to **1e** starting from chloride **4c** (45 mg, 0.1 mmol) and 2-methylpropylamine (74 mg, 0.5 mmol). Yield: 40 mg, 75%. ¹H NMR (400 MHz, MeOD₄, rotameric): δ 8.01 (m, 1H), 7.71 (m, 1H), 7.38 (m, 1H), 4.68 (m, 1H), 3.98 (s, 1H), 3.45 (m, 2H), 3.34 (s, 3H), 2.35 (s, 3H), 2.13–1.88 (m, 3H), 1.25–0.75 (m, 6H). HPLC: *t*_R = 2.03 min, 98.0% purity. HRMS (EI): *m/z* calcd for C₁₉H₂₈N₈O [M + H]⁺ 385.2464, found 385.2471.

(S)-3-(4-(Isopropyl(methyl)amino)-6-(pyrrolidin-3-ylamino)-1,3,5-triazin-2-ylamino)-4-methylbenzamide Trifluoroacetate (1h). **1h** was prepared similarly to **1e** starting from chloride **4c** (50 mg, 0.2 mmol) and 1-methylpropyl(methyl)amine (74 mg, 0.5 mmol). Yield: 13 mg, 22%. ¹H NMR (400 MHz, MeOD₄, rotameric): δ 8.00 (m, 1H), 7.75 (s, 1H), 7.41 (d, *J* = 7.7 Hz, 1H), 4.72 (m, 1H), 4.00 (s, 1H), 3.64–3.62 (m, 8H), 2.38–1.97 (m, 6H), 1.28–0.98 (m, 6H). HPLC: *t*_R = 2.28 min, 96.8% purity. HRMS (EI): *m/z* calcd for C₂₀H₃₀N₈O [M + H]⁺ 399.2621, found 399.2621.

(S)-4-Methyl-3-(4-(methyl(neopentyl)amino)-6-(pyrrolidin-3-ylamino)-1,3,5-triazin-2-ylamino)benzamide Trifluoroacetate (1i). **1i** was prepared similarly to **1e** starting from chloride **4c** (45 mg, 0.1 mmol) and neopentyl(methyl)amine (74 mg, 0.5 mmol). Yield: 27 mg, 45%. ¹H NMR (400 MHz, MeOD₄, rotameric): δ 8.05 (m, 1H), 7.76 (m, 1H), 7.41 (m, 1H), 4.77 (m, 1H), 3.99 (s, 1H), 3.67–3.16 (m, 8H), 2.44 (m, 1H), 2.35 (s, 3H), 2.20 (m, 1H), 0.98–0.79 (m, 9H). HPLC: *t*_R = 2.49 min, 99.4% purity. HRMS (EI): *m/z* calcd for C₂₁H₃₂N₈O [M + H]⁺ 413.2777, found 413.2773.

(S)-3-(4-(Cyclohexyl(methyl)amino)-6-(pyrrolidin-3-ylamino)-1,3,5-triazin-2-ylamino)-4-methylbenzamide Trifluoroacetate(1j). **1j** was prepared similarly to **1e** starting from chloride **4c** (45 mg, 0.1 mmol) and cyclohexyl(methyl)amine (74 mg, 0.5 mmol). Yield: 23 mg, 39%. ¹H NMR (400 MHz, MeOD₄, rotameric): δ 8.21 (m, 1H), 7.73 (s, 1H), 7.41 (s, 1H), 4.68 (m, 2H), 3.63–3.34 (m, 4H), 3.06 (m, 2H), 2.42 (s, 1H), 2.38 (s, 3H), 2.19 (br s, 1H). 1.88–1.22 (m, 11H). HPLC:

$t_R = 2.02$ min, 97.8% purity. HRMS (EI): m/z calcd for $C_{22}H_{32}N_8O$ $[M + H]^+$ 425.2777, found 425.2775.

N-Methoxy-4-methyl-3-(4-(methyl(neopentyl)amino)-6-(4-methylpiperazin-1-yl)-1,3,5-triazin-2-ylamino)benzamide Trifluoroacetate (1k). This compound was prepared according to the procedure for **1b** starting with **4a** and methylpiperazine. Yield: 65%, white solid. 1H NMR (400 MHz, MeOD₄, appears as 2 rotamers): δ 8.34, 8.14 (s, 1H), 7.33–7.31 (m, 1H), 7.23–7.21 (m, 1H), 3.70 (s, 3H), 3.47–3.02 (m, 13H), 2.84 (s, 3H), 2.27, 2.23 (s, 3H), 0.91, 0.80 (s, 9H). HPLC: $t_R = 2.28$ min, 98% purity. HRMS (EI): m/z calcd for $C_{23}H_{37}N_8O_2$ $[M + H]^+$ 457.3039, found 457.3033.

N-Methoxy-4-methyl-3-(4-(methyl(neopentyl)amino)-6-(piperazin-1-yl)-1,3,5-triazin-2-ylamino)benzamide Trifluoroacetate (1l). This compound was prepared according to the procedure for **1b** starting with **4a** and piperazine: white solid in 46% yield. 1H NMR (400 MHz, MeOD₄, appears as 2 rotamers): δ 8.37, 8.16 (s, 1H), 7.32–7.30 (m, 1H), 7.23–7.21 (m, 1H), 3.96 (app t, $J = 5.1$ Hz, 4H), 3.70 (s, 3H), 3.47, 3.35 (s, 2H), 3.19 (app t, $J = 5.3$ Hz, 4H), 3.12, 3.08 (s, 3H), 2.28, 2.24 (s, 3H), 0.91, 0.80 (s, 9H). HPLC: $t_R = 2.27$ min, 99% purity. HRMS (EI): m/z calcd for $C_{22}H_{35}N_8O_2$ $[M + H]^+$ 443.2883, found 443.2894.

N-Methoxy-4-methyl-3-(4-(methyl(neopentyl)amino)-6-(4-methyl-1,4-diazepan-1-yl)-1,3,5-triazin-2-ylamino)benzamide Trifluoroacetate (1m). This compound was prepared according to the procedure for **1b** starting with **4a** and 4-methyl-1,4-diazepan. Yield: 68% of a white solid. 1H NMR (400 MHz, MeOD₄, appears as 2 rotamers): δ 8.57, 8.40 (br s, 1H), 7.45–7.43 (m, 1H), 7.36–7.34 (m, 1H), 4.36–4.32 (m, 1H), 4.10–3.89 (m, 2H), 3.83 (s, 3H), 3.78–3.71 (m, 1H), 3.65–3.50 (m, 2H), 3.35–3.22 (m, 7H), 2.98 (s, 3H), 2.44–2.41 (m, 3H), 2.30 (br s, 2H), 1.05 (br s, 9H). HPLC: $t_R = 2.09$ min, >99% purity. HRMS (EI): m/z calcd for $C_{24}H_{38}N_8O_2$ $[M + H]^+$ 471.3118, found 471.3192.

3-(4-(1,4-Diazepan-1-yl)-6-(methyl(neopentyl)amino)-1,3,5-triazin-2-ylamino)-N-methoxy-4-methylbenzamide Trifluoroacetate (1n). This compound was prepared according to the procedure for **1b** starting with **4a** and 1,4-diazepan: 68%, white solid. 1H NMR (400 MHz, MeOD₄, appears as 2 rotamers): δ 8.53, 8.30 (br s, 1H), 7.46–7.45 (m, 1H), 7.37–7.35 (m, 1H), 4.15–3.70 (m, 4H), 3.61–3.35 (m, 4H), 3.27–3.24 (m, 3H), 2.41–2.38 (m, 3H), 2.18 (m, 2H), 1.05, 0.93 (s, 9H). HPLC: $t_R = 2.28$ min, >99% purity. HRMS (EI): m/z calcd for $C_{23}H_{37}N_8O_2$ $[M + H]^+$ 457.3039, found 457.3027.

Methyl 3-(4,6-Dichloro-1,3,5-triazin-2-ylamino)-4-methylbenzoate (6). To a solution of 5.7 g (33 mmol) of aniline **5** in acetone (120 mL) at 0 °C was added 6.0 g (32.5 mmol) of cyanuric chloride. The resulting mixture was allowed to warm to room temperature giving, a thick suspension, which was stirred for 1 h before addition of crushed ice (~100 mL). The mixture was stirred for 20 min, then water (100 mL) was added, and the solid was collected by vacuum filtration. The solid was washed with additional water (3 × 100 mL), and the solid was dried in vacuo to afford 9.95 g (98%) of **6** as a white solid. 1H NMR (400 MHz, DMSO-*d*₆): δ 10.80 (s, 1H), 7.91 (d, $J = 1.3$ Hz, 1H), 7.81 (dd, $J = 7.9, 1.6$ Hz, 1H), 7.46 (d, $J = 8.0$ Hz, 1H), 3.85 (s, 3H), 2.28 (s, 3H). HPLC: $t_R = 3.15$ min, 99% purity. HRMS (EI): m/z calcd for $C_{12}H_{11}N_4O_2Cl_2$ $[M + H]^+$ 313.0259, found 313.0253.

Methyl 3-(4-Chloro-6-(methyl(neopentyl)amino)-1,3,5-triazin-2-ylamino)-4-methylbenzoate (8). This compound was prepared using the general procedure described for compound **3a** to afford the title compound as a white solid: 98% yield. 1H NMR (400 MHz, MeOD₄): δ 8.23 (s, 1H), 7.78–7.74 (m, 1H), 7.38–7.34 (m, 1H), 3.90 (s, 3H), 3.52, 3.41 (s, 2H), 3.16, 3.14 (s, 3H), 2.37, 2.35 (s, 3H), 0.99, 0.81 (s, 9H). HPLC: $t_R = 4.08$ min, >99% purity. HRMS (EI): m/z calcd for $C_{18}H_{25}N_5O_2Cl$ $[M + H]^+$ 378.1697, found 378.1700.

(R)-3-(4-(1-(tert-Butoxycarbonyl)pyrrolidin-3-ylamino)-6-(methyl(neopentyl)amino)-1,3,5-triazin-2-ylamino)-4-methylbenzoic acid (10). A solution of 3.0 g (8.0 mmol) of **8**, 2.1 mL (12 mmol) of DIPEA, and 1.8 g (9.5 mmol) of (R)-3-amino-1-*N*-Boc-pyrrolidine (**9**) in NMP (10 mL) was heated

to 140 °C for 4 h. The resulting mixture was cooled to room temperature and added dropwise with stirring to a mixture of an aqueous saturated solution of ammonium chloride (50 mL) diluted with water (50 mL). The resulting solid was collected by vacuum filtration and washed with water (3 × 75 mL) and allowed to partially air-dry. The moist solid was dissolved in methanol (50 mL), 3 N aqueous sodium hydroxide (13 mL) was added, and the solution was heated to 60 °C for 45 min. After cooling to room temperature, the methanol was removed using a rotary evaporator and the resulting aqueous solution was diluted with additional water (~100 mL). The solution was acidified to pH 4 by addition of 10% aqueous citric acid solution (~100 mL), and the resulting gelatinous precipitate was collected by vacuum filtration. The solid was washed with water (2 × 50 mL) and ethyl acetate (2 × 50 mL) and then dried in vacuo overnight to afford 3.2 g (79%) of **10** as a white powder. 1H NMR (400 MHz, DMSO-*d*₆, appears as 2 rotamers): δ 12.50 (br s, 1H), 8.17–8.09 (m, 2H), 7.57 (m, 1H), 7.28 (d, $J = 7.9$ Hz, 1H), 7.05–6.94 (m, 1H), 4.36–4.26 (m, 1H), 3.57–3.23 (m, 6H), 3.05 (s, 3H), 2.27 (br s, 3H), 2.04 (br s, 1H), 1.84 (br s, 1H), 1.39, 1.38 (s, 9H), 0.93, 0.79 (s, 9H). HPLC: $t_R = 3.83$ min, 95% purity.

General Procedure for the Synthesis of Compounds 11a–i. A solution of 0.10 g (0.20 mmol) of **10**, EDCI (0.25 mmol), and HOBt (0.23 mmol) in DMF (0.4 mL) was stirred at room temperature for 2 h, and then DIPEA (0.58 mmol) and the amine R₁R₂NH (0.58 mmol) or its hydrochloride salt were added. After stirring at room temperature for 16 h, water (5 mL) and saturated aqueous NaHCO₃ solution (1 mL) were successively added. The desired intermediate compounds were isolated either by vacuum filtration and washing with water (3 × 1 mL) or by extraction with ethyl acetate and concentration in vacuo. Further drying in vacuo afforded a solid, which was dissolved in anhydrous dioxane (1 mL). To this solution was added a 4 N solution of anhydrous HCl in dioxane (0.5 mL), and the resulting solution was stirred at room temperature for 15 h. The solvent was removed in vacuo, and the resulting semisolid was dissolved in methanol (~1 mL) and subjected to purification by reverse-phase HPLC chromatography. The HPLC fractions containing the purified product were concentrated on a rotary evaporator to remove the methanol solvent, and the resulting aqueous solutions were lyophilized to afford the title compounds **11a–h**.

(S)-N-Ethyl-4-methyl-3-(4-(methyl(neopentyl)amino)-6-(pyrrolidin-3-ylamino)-1,3,5-triazin-2-ylamino)benzamide Trifluoroacetate (11a). Yield: 69%. 1H NMR (400 MHz, MeOD₄, appears as 2 rotamers): δ 8.12, 7.96 (s, 1H), 7.69–7.65 (m, 1H), 7.41–7.39 (m, 1H), 4.75 (br s, 1H), 3.63–3.40 (m, 8H), 3.25–3.20 (m, 3H), 2.39–2.35 (m, 4H), 2.18 (m, 1H), 1.24 (t, $J = 7.2$ Hz, 3H), 1.04, 0.82 (s, 9H). HPLC: $t_R = 2.26$ min, >99% purity. HRMS (EI): m/z calcd for $C_{23}H_{37}N_8O$ $[M + H]^+$ 441.3090, found 441.3076.

(S)-N-(2-Methoxyethyl)-4-methyl-3-(4-(methyl(neopentyl)amino)-6-(pyrrolidin-3-ylamino)-1,3,5-triazin-2-ylamino)benzamide Trifluoroacetate (11b). Yield: 23%. 1H NMR (400 MHz, MeOD₄, appears as 2 rotamers): δ 8.03, 7.86 (br s, 1H), 7.57–7.52 (m, 1H), 7.28 (m, 1H), 4.77–4.74 (m, 1H), 3.51–3.25 (m, 13H), 3.12–3.08 (m, 3H), 2.27–2.23 (m, 4H), 2.06 (m, 1H), 0.92, 0.71 (s, 9H). HPLC: $t_R = 2.55$ min, >99% purity. HRMS (EI): m/z calcd for $C_{24}H_{39}N_8O_2$ $[M + H]^+$ 471.3196, found 471.3201.

(S)-N-Benzyl-4-methyl-3-(4-(methyl(neopentyl)amino)-6-(pyrrolidin-3-ylamino)-1,3,5-triazin-2-ylamino)benzamide Trifluoroacetate (11c). Yield: 57%. 1H NMR (400 MHz, MeOD₄, appears as 2 rotamers): δ 8.19, 8.00 (br s, 1H), 7.74–7.69 (m, 1H), 7.41–7.25 (m, 6H), 4.73 (m, 1H), 4.59 (s, 3H), 3.62–3.38 (m, 6H), 3.23–3.15 (m, 3H), 2.39–2.35 (m, 4H), 2.17 (m, 1H), 1.03, 0.78 (s, 9H). HPLC: $t_R = 2.77$ min, >99% purity. HRMS (EI): m/z calcd for $C_{28}H_{39}N_8O$ $[M + H]^+$ 503.3247, found 503.3242.

(S)-Methyl-4-methyl-3-(4-(methyl(neopentyl)amino)-6-(pyrrolidin-3-ylamino)-1,3,5-triazin-2-ylamino)benzamide Trifluoroacetate (11d). Yield: 27%, off-white solid. 1H NMR (400 MHz, DMSO-*d*₆, appears as 2 rotamers): δ 8.60,

8.37 (br s, 1H), 7.54 (m, 1H), 7.20–7.17 (m, 1H), 4.38 (m, 1H), 3.77 (s, 3H), 3.45–3.34 (m, 2H), 3.20–2.96 (m, 7H), 2.24 (s, 3H), 2.13, 1.80 (br s, 2H), 0.83, 0.75 (br s, 9H). HPLC: t_R = 2.72 min, >99% purity. HRMS (EI): m/z calcd for $C_{22}H_{33}N_7O_2$ [M + H]⁺ 428.2767, found 428.2774.

(S)-N-Cyclopentyl-4-methyl-3-(4-(methyl(neopentyl)amino)-6-(pyrrolidin-3-ylamino)-1,3,5-triazin-2-ylamino)benzamide Trifluoroacetate (11e). Yield: 62%. ¹H NMR (400 MHz, MeOD₄, appears as 2 rotamers): δ 8.00, 7.85 (br s, 1H), 7.56–7.54 (m, 1H), 7.28–7.26 (m, 1H), 4.74–4.62 (m, 1H), 4.24–4.19 (m, 1H), 3.51–3.23 (m, 6H), 3.12–3.03 (m, 3H), 2.26–2.22 (m, 4H), 2.05 (m, 1H), 2.05–1.88 (m, 2H), 1.68–1.66 (m, 2H), 1.58–1.44 (m, 4H), 0.92, 0.71 (s, 9H). HPLC: t_R = 2.71 min, >99% purity. HRMS (EI): m/z calcd for $C_{14}H_{18}NO_5$ [M + H]⁺ 481.3403, found 481.3395.

(S)-N-Methoxy-4-methyl-3-(4-(methyl(neopentyl)amino)-6-(pyrrolidin-3-ylamino)-1,3,5-triazin-2-ylamino)benzamide Trifluoroacetate (11f). Yield: 85%. ¹H NMR (400 MHz, MeOD₄, appears as 2 rotamers): δ 8.15, 7.97 (br s, 1H), 7.58 (m, 1H), 7.42–7.40 (m, 1H), 4.69 (m, 1H), 3.82 (s, 3H), 3.66–3.44 (m, 6H), 3.24 (m, 3H), 2.39–2.36 (m, 4H), 2.18 (m, 1H), 1.04, 0.83 (s, 9H). HPLC: t_R = 2.20 min, 98% purity. HRMS (EI): m/z calcd for $C_{22}H_{35}N_8O_2$ [M + H]⁺ 443.2883, found 443.2881.

(S)-N-Hydroxy-4-methyl-3-(4-(methyl(neopentyl)amino)-6-(pyrrolidin-3-ylamino)-1,3,5-triazin-2-ylamino)benzamide Trifluoroacetate (11g). Yield: 55%. ¹H NMR (400 MHz, MeOD₄, appears as 2 rotamers): δ 8.01, 7.80 (br s, 1H), 7.47–7.27 (m, 2H), 4.56 (br s, 1H), 3.52–3.31 (m, 6H), 3.12–3.09 (m, 3H), 2.27–2.23 (m, 4H), 2.06 (br s, 1H), 0.92, 0.71 (s, 9H). HPLC: t_R = 1.89 min, >99% purity. HRMS (EI): m/z calcd for $C_{21}H_{33}N_8O_2$ [M + H]⁺ 429.2726, found 429.2720.

(S)-N-Isopropyl-4-methyl-3-(4-(methyl(neopentyl)amino)-6-(pyrrolidin-3-ylamino)-1,3,5-triazin-2-ylamino)benzamide Trifluoroacetate (11h). Yield: 88%. ¹H NMR (400 MHz, MeOD₄, appears as 2 rotamers): δ 7.95, 7.70 (s, 1H), 7.66 (m, 1H), 7.40 (m, 1H), 4.76 (m, 1H), 4.22 (m, 1H), 3.64–3.40 (m, 6H), 3.28–3.19 (m, 3H), 2.38–2.34 (m, 4H), 2.22–2.18 (m, 1H), 1.26 (d, J = 6.6 Hz, 6H), 1.04, 0.81 (s, 9H). HPLC: t_R = 2.38 min, >99% purity. HRMS (EI): m/z calcd for $C_{24}H_{39}N_8O$ [M + H]⁺ 455.3247, found 455.3236.

Generation of p38 kinases. cDNAs of human p38 α , β isozymes were cloned using PCR technology. These cDNAs were subcloned in the pGEX expression vector (Pharmacia). GST-p38 fusion protein was expressed in *Escherichia coli* and purified from bacterial pellets by affinity chromatography using glutathione agarose. p38 fusion protein was activated by incubating with constitutively active MKK6. Active p38 was separated from MKK6 by affinity chromatography. Phosphorylated MKK6 was generated according to the literature.⁹

p38 Kinase Assay. The assay were performed in V-bottomed 96-well plates. For both assays, the final assay volume was 60 μ L which was from three 20- μ L additions of enzyme, substrates (myelin basic protein (MBP) and ATP), and test compounds in assay buffer (50 mM Tris pH 7.5, 10 mM MgCl₂, 50 mM NaCl, and 1 mM DTT). Bacterially expressed, activated p38 was preincubated with test compounds for 10 min prior to the initiation of reaction by adding substrates. The plates were incubated at room temperature for 45 min. The reaction was terminated by adding 5 μ L of 0.5 M EDTA to each well. The reaction mixture was aspirated onto a prewetted filtermat using a Skatron Micro96 cell harvester (Skatron) and then washed with PBS. The filtermat was dried in a microwave oven for 1 min, coated with a layer of MeltiLex A scintillation wax (PerkinElmer), and counted on a Microbeta scintillation counter (Model 1450, PerkinElmer). The data were analyzed using the Prizm nonlinear least-squares regression (GraphPad Software). The final concentrations of reagents in the assays were [ATP], 1 μ M; [γ -³³P]ATP], 3 nM; [MBP] (Sigma, M1891), 2 μ g/well; [p38], 15 ng/well; [DMSO], 0.3%.

LPS-Induced TNF Production in THP-1 Cells. Human monocytic THP-1 cells, obtained from ATCC, were maintained in RPMI 1640 medium supplemented with 10% fetal bovine serum. Cells (40000 cells in 80 μ L) were added to wells of 96-

well flat-bottomed plates. Tested compounds (10 μ L) or vehicle (1% DMSO final) was added to cells. Subsequently, LPS (Sigma, No. L7261; 10 μ L/well) was added to the cells for a final concentration of 1 μ g/mL. Plates were incubated overnight at 37 °C and 5% CO₂. Supernatant (50 μ L/well) was harvested for an ELISA assay. TNF was captured by an anti-human TNF antibody (R&D, No. MAB610) which was preabsorbed in high binding EIA plates (Costar, No. 3590). Captured TNF was recognized by a biotinylated anti-human TNF polyclonal antibody (R&D, No. BAF210). Streptavidin conjugated with peroxidase was added to each well, and the activity of peroxidase was quantitated by a peroxide substrate kit (Pierce, No. 34062 and No. 34006).

LPS-Induced TNF Production in Human PBMC. Human PBMCs were isolated from whole blood collected from healthy donors. Blood was diluted into RPMI 1640 (Life Technologies) containing 2.5 mM EDTA (Life Technologies) and 10 μ g/mL polymyxin (Sigma), then underlaid with ficoll (Accurate Scientific Co.), and centrifuged at 600g for 25 min. The interface was collected, and cells were washed twice and resuspended in RPMI, 10% FBS. Cells were then distributed (200 μ L/well) into 96-well tissue culture treated plates (Falcon) at 1×10^6 cells/mL in RPMI, 10% FBS. Test compounds were added to appropriate wells and incubated with cells for 30 min. Cells were then stimulated by the addition of lipopolysaccharide (LPS, BioWhittaker), with a final concentration of 25 ng/mL, and incubated for 6 h at 37 °C, 5% CO₂. The cell supernatants were removed and assayed for TNF- α by ELISA (R&D Systems).

Cytotoxicity Assay. T cells in 1.25×10^6 /mL human peripheral blood mononuclear cells (PBMC) isolated from normal volunteers were stimulated with 5 μ g/mL phytohemagglutinin (PHA) for 4 days to generate dividing T cell blasts. The PHA blast cells at 1.5×10^6 per mL were incubated with 30 μ M compound in RPMI media (Gibco) with 10% fetal bovine serum and a final dimethyl sulfoxide concentration of 0.003% for 24 h at 37 °C, 5% CO₂. Cytotoxicity was determined by the detection of metabolic activity using the AlamarBlue assay (Biosource).¹⁰

Inhibition of TNF- α Release in Mice. BALB/c female mice, 6–8 weeks of age, were obtained from Harlan Laboratories and maintained ad libitum on water and standard rodent chow (Harlan Teklad). Mice were acclimated to ambient conditions for at least one week prior to use. For oral dosing, the compounds were prepared in a solution of 100% polyethylene glycol (MW 300) and a dosing volume of 0.2 mL per mouse was administered by gavage 30 min prior to LPS injection (0.1 mL of LPS suspended at 10 μ g/mL in PBS, administered ip). Blood samples were obtained 90 min after LPS injection. Serum was separated from clotted blood samples by centrifugation (5 min, 5000g, room temperature) and analyzed for levels of TNF- α by ELISA assay (R&D Systems) according to the manufacturer's directions. Results are shown as mean \pm SD of n = 8 mice per treatment group. All procedures involving animals were reviewed and approved by the Institutional Animal Care and Use Committee.

Rat Adjuvant Arthritis. Male Lewis rats (Harlan, 175–200 g) were immunized sc at the base of the tail with 0.1 mL complete Freund's adjuvant containing 10 mg/mL *Mycobacterium butyricum*. Seven days later, baseline (predisease) measurements of hind paw volume were determined by volume displacement plethysmometry (Ugo Basile, Italy). Compound was administered orally at 1 mL b.i.d. beginning on day 11. Paw volume measurements were repeated 3 \times /week for the remainder of the study. Data are presented as the summed increase in volume (expressed in milliliters) above baseline for each rat's two hind paws.

Crystal Structure of p38 MAP Kinase. His-p38 MAP kinase was expressed in *E. coli* (BL21 DE3) and purified by sequential anion exchange, nickel chelate affinity, and size exclusion chromatography. The protein at 2 mg/mL, in 25 mM Tris (pH 7.4), 50 mM NaCl, 5% glycerol, 2mM DTT, was complexed with a 5-fold molar excess of **1m** and then concentrated to 17 mg/mL. Crystals of p38 MAP kinase were grown

Table 6. Crystallographic Data Collection, Reduction, and Refinement

temperature	100 °K
detector	Rigaku R-AXIS IV area detector
source	Rigaku RU-2000 rotating anode
max obsd resolution	2.2 Å
Data Reduction (10.0–2.2 Å)	
data reduction program	HKL (Denzo)
completeness	99.7%
Rsymm (on intensity)	10.2%
reflections collected	63975
no. of unique reflections	19798
average $I(\sigma I)$	10.7
data redundancy	3.2
real space cell <i>a</i>	65.81 Å
real space cell <i>b</i>	74.45 Å
real space cell <i>c</i>	78.26 Å
space group	<i>P</i> 212121
Refinement Procedure	
refinement program	CNX 2000
completeness	99.3%
no. of reflections used	19748
<i>R</i> value	29.9%
free <i>R</i> value	35.1%
no. of atoms used	2732
protein atoms	2653
inhibitor atoms	34
solvent molecules	45
estimate <i>B</i> value (Wilson plot)	42.7 Å ²
mean <i>B</i> value	41.3 Å ²
ESD coordinate error (Luzzati plot)	0.38 Å
RMS deviations from ideal values	
bond lengths	0.007 Å
bond angles	1.3°
dihedral angles	22.8°
improper angles	0.8

by the hanging drop method from solutions containing 30% PEG 10K, 5 mM MgSO₄, 50 mM MES, pH 6.0. Data were collected to approximately 2.2 Å resolution on the R-AXIS IV area detector, reduced using the Denzo/HKL package, and refined by the method of simulated annealing using program CNX. The crystallographic data collection, reduction, and refinement are summarized in Table 6.

References

- (1) (a) Dinarello, C. A. Inflammatory cytokines: Interleukin-1 and tumor necrosis factor as effector molecules in autoimmune diseases. *Curr. Opin. Immunol.* **1991**, *3*, 941–948. (b) Arend, W. P.; Dayer, J. M. Cytokines and cytokine inhibitors or antagonists in rheumatoid arthritis. *Arthritis Rheum.* **1990**, *33*, 305–315. (c) Dayer, J. M.; Demczuk, S. Cytokines and other mediators in rheumatoid arthritis. *Springer Semin. Immunopathol.* **1984**, *7*, 387–413.
- (2) (a) Moreland, L. W. Drugs that block tumor necrosis factor: experience in patients with rheumatoid arthritis. *Pharmacoeconomics* **2004**, *22* (2, Suppl.), 39–53. (b) Bresnihan, B. Interleukin-1 receptor antagonist treatment in rheumatoid arthritis. *Mod. Ther. Rheum. Dis.* **2002**, 109–120. (c) Elliott, M. J.; Feldmann, M.; Maini, R. N. TNF α blockade in rheumatoid arthritis: rationale, clinical outcomes and mechanisms of action. *Int. J. Immunopharmacol.* **1995**, *17* (2), 141–145. (d) Feldmann, M.; Elliott, M. J.; Brennan, F. M.; Maini, R. N. Use of anti-tumor necrosis factor antibodies in rheumatoid arthritis. *J. Interferon Res.* **1994**, *14* (5), 299–300.
- (3) (a) Cobb, M. H.; Goldsmith, E. J. How MAP kinases are regulated. *J. Biol. Chem.* **1995**, *270* (25), 14843–14846. (b) Gille, H.; Sharrocks, A. D.; Shaw, P. E. Phosphorylation of transcription factor p62TCF by MAP kinase stimulates ternary complex formation at *c-fos* promoter. *Nature* **1992**, *358* (6385), 414–417.
- (4) Lee, J. C.; Kassis, S.; Kumar, S.; Badger, A.; Adams, J. L. p38 mitogen-activated protein kinase inhibitors—mechanisms and therapeutic potentials. *Pharmacol. Ther.* **1999**, *82* (2–3), 389–397.
- (5) Behr, T. M.; Berova, M.; Doe, C. P.; Ju, H.; Angermann, C. E.; Boehm, J.; Willette, R. N. p38 mitogen-activated protein kinase inhibitors for the treatment of chronic cardiovascular disease. *Curr. Opin. Invest. Drugs (PharmaPress Ltd.)* **2003**, *4* (9), 1059–1064 and references therein.
- (6) (a) Regan, J.; Breitfelder, S.; Cirillo, P.; Gilmore, T.; Graham, A. G.; Hickey, E.; Klaus, B.; Madwed, J.; Moriaki, M.; Moss, N.; Pargellis, C.; Pav, S.; Proto, A.; Swinamer, A.; Tong, L.; Torcellini, C. Pyrazole Urea-Based Inhibitors of p38 MAP Kinase: From Lead Compound to Clinical Candidate. *J. Med. Chem.* **2002**, *45* (14), 2994–3008. (b) Branger, J.; Van den Blink, B.; Weijer, S.; Madwed, J.; Bos, C. L.; Gupta, A.; Yong, C.; Polmar, S. H.; Olszyna, D. P.; Hack, C. E.; Van D., Sander J. H.; Peppelenbosch, M. P.; Van der Poll, T. Anti-inflammatory effects of a p38 mitogen-activated protein kinase inhibitor during human endotoxemia. *J. Immunol.* **2002**, *168* (8), 4070–4077. (c) Reference 5.
- (7) (a) Shewchuk, L.; Hassell, A.; Wisely, B.; Rocque, W.; Holmes, W.; Veal, J.; Kuyper, L. F. Binding mode of the 4-anilinoquinazoline class of protein kinase inhibitor: X-ray crystallographic studies of 4-anilinoquinazolines bound to cyclin-dependent kinase 2 and p38 kinase. *J. Med. Chem.* **2000**, *43* (1), 133–138. (b) Henry, J. R.; Cavender, D. E.; Wadsworth, D. A. p38 Mitogen Activated Protein Kinase as a Target for Drug Discovery. *Drugs Future* **1999**, *24*, 1345–1354. (c) Salituro, F. G.; Germann, U. A.; Wilson, K. P.; Bemis, G. W.; Fox, T.; Su, M. S. Inhibitors of p38 MAP kinase: therapeutic intervention in cytokine-mediated diseases. *Curr. Med. Chem.* **1999**, *6*, 807–823. Reference 6a.
- (8) Moriarty, K.; Shimshock, Y.; Ahmed, G.; Wu, J.; Wen, J.; Li, W.; Erickson, S.; Letourneau, J.; McDonald, E.; Leftheris, K.; Wroblewski, S. T.; Hussain, Z.; Henderson, I.; Metzger, A.; Baldwin, J. J.; Dyckman, A. J. Preparation of *s*-triazines and pyrimidines for pharmaceutical use as cytokine, especially TNF- α , inhibitors. U.S. Pat. Appl. Publ., **2002**, Cont.-in-part US 2002137747 A1.
- (9) Raingeaud, J.; Whitmarsh, A. J.; Barrett, T.; Derijard, B.; Davis, R. J. MKK3- and MKK6-regulated gene expression is mediated by the p38 mitogen-activated protein kinase signal transduction pathway. *Mol. Cell. Biol.* **1996**, *16* (3), 1247–1255.
- (10) (a) Fields, R. D.; Lancaster, M. V. Dual attribute continuous monitoring of cell proliferation/cytotoxicity. *Am. Biotechnol. Lab.* **1993**, *11* (4), 48–50. (b) Ahmed, S. A.; Gogal, R. M., Jr.; Walsh, J. E. A new rapid and simple nonradioactive assay to monitor and determine the proliferation of lymphocytes: an alternative to H³-thymidine incorporation assay. *J. Immunol. Methods* **1994**, *170*, 211–224.

JM049521D